

NAVAL POSTGRADUATE SCHOOL

Monterey, California



DTIC QUALITY INSPECTED 2

THESIS

THE MACH-ZEHNDER COUPLER

by

Maryanne Heinbaugh

March 1997

Thesis Co-Advisors:

John P. Powers
Tri Ha

Approved for public release; distribution is unlimited.

19970827 120

REPORT DOCUMENTATION PAGE			Form Approved OMB No. 0704-0188	
Public reporting burden for this collection of information is estimated to average 1 hour per response, including the time for reviewing instruction, searching existing data sources, gathering and maintaining the data needed, and completing and reviewing the collection of information. Send comments regarding this burden estimate or any other aspect of this collection of information, including suggestions for reducing this burden, to Washington Headquarters Services, Directorate for Information Operations and Reports, 1215 Jefferson Davis Highway, Suite 1204, Arlington, VA 22202-4302, and to the Office of Management and Budget, Paperwork Reduction Project (0704-0188) Washington DC 20503.				
1. AGENCY USE ONLY (Leave blank)		2. REPORT DATE March 1997		3. REPORT TYPE AND DATES COVERED Master's Thesis
4. TITLE AND SUBTITLE The Mach-Zehnder Coupler			5. FUNDING NUMBERS	
6. AUTHOR(S) Heinbaugh, Maryanne				
7. PERFORMING ORGANIZATION NAME(S) AND ADDRESS(ES) Naval Postgraduate School Monterey CA 93943-5000			8. PERFORMING ORGANIZATION REPORT NUMBER	
9. SPONSORING/MONITORING AGENCY NAME(S) AND ADDRESS(ES) Naval Postgraduate School Monterey CA 93943-5000			10. SPONSORING/MONITORING AGENCY REPORT NUMBER	
11. SUPPLEMENTARY NOTES The views expressed in this thesis are those of the author and do not reflect the official policy or position of the Department of Defense or the U.S. Government.				
12a. DISTRIBUTION/AVAILABILITY STATEMENT Approved for public release; distribution is unlimited.			12b. DISTRIBUTION CODE	
13. ABSTRACT (maximum 200 words) At the Naval Postgraduate School (NPS) we are currently researching the potential for and feasibility of an optical signal demultiplexer based on the Mach-Zehnder coupler. The theory behind the signal demultiplexer involves cascading an n stage Mach-Zehnder coupler. The coupler will be capable of discriminating between M different CSK signals employing M Hadamard code. This thesis involves the examination of a single Mach-Zehnder coupler that operates at 100 Mbps and specifically addresses the mathematical analysis of how it operates, the physical components necessary to build and test a Mach-Zehnder coupler, and the performance of the Mach-Zehnder coupler.				
14. SUBJECT TERMS Mach-Zehnder coupler, fiber optic signal demultiplexing.			15. NUMBER OF PAGES 60	
			16. PRICE CODE	
17. SECURITY CLASSIFICATION OF REPORT Unclassified	18. SECURITY CLASSIFICATION OF THIS PAGE Unclassified	19. SECURITY CLASSIFICATION OF ABSTRACT Unclassified	20. LIMITATION OF ABSTRACT UL	

Approved for public release; distribution is unlimited

THE MACH-ZEHNDER COUPLER

Maryanne Heinbaugh
Lieutenant, United States Navy
B.A., University of Washington, 1986

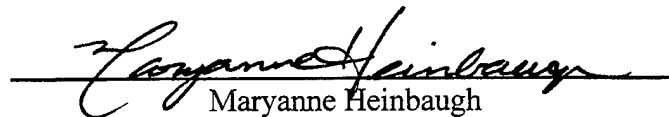
Submitted in partial fulfillment of the
requirements for the degree of

MASTER OF SCIENCE IN ELECTRICAL ENGINEERING

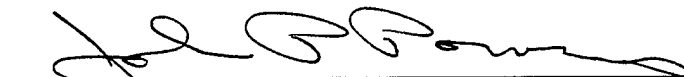
from the


NAVAL POSTGRADUATE SCHOOL
March 1997

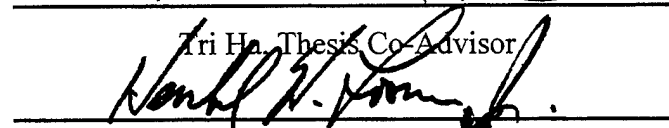
Author


Maryanne Heinbaugh

Approved by:


John P. Powers, Thesis Co-Advisor


Tri T. Ha, Thesis Co-Advisor


Herschel H. Loomis, Jr., Chairman
Department of Electrical
Engineering

ABSTRACT

At the Naval Postgraduate School (NPS) we are currently researching the potential for and feasibility of an optical signal demultiplexer based on the Mach-Zehnder coupler. The theory behind the signal demultiplexer involves cascading an n stage Mach-Zehnder coupler. The coupler will be capable of discriminating between M different CSK signals employing M Hadamard codes. This thesis involves the examination of a single Mach-Zehnder coupler that operates at 100 Mbps and specifically addresses the mathematical analysis of how it operates, the physical components necessary to build and test a Mach-Zehnder coupler, and the performance of the Mach-Zehnder coupler.

TABLE OF CONTENTS

I.	INTRODUCTION	1
II.	THE MACH-ZEHNDER COUPLER.....	5
A.	OVERVIEW OF THE MACH-ZEHNDER COUPLER	5
B.	ANALYTICAL DESCRIPTION OF COMPONENTS.....	6
1.	2x2 Coupler.....	6
2.	Delay Line.....	9
3.	Phase Shifter	9
C.	SIGNAL ANALYSIS OF THE MACH-ZEHNDER COUPLER.....	9
D.	SUMMARY.....	12
III.	HARDWARE DESCRIPTION	15
A.	2x2 COUPLER	15
1.	Insertion Loss	16
2.	Time Delay.....	19
B.	DELAY LINE.....	24
1.	Fiber Length.....	24
2.	Insertion Loss.....	25
3.	Time Delay.....	26
C.	$\pi/2$ PHASE SHIFTER	26
D.	ATTENUATOR.....	28
1.	Insertion Loss.....	29
E.	THE MACH-ZEHNDER COUPLER.....	29
1.	Setup	33
2.	Results.....	37
IV	DISCUSSION AND CONCLUSIONS	39
APPENDIX A. DETAILED DESCRIPTION OF EQUIPMENT AND PROCEDURE USED FOR MEASURING INSERTION LOSSES		43
APPENDIX B. DETAILED DESCRIPTION OF PROCEDURE USED FOR MEASURING THE TIME DELAY.....		45
LIST OF REFERENCES		47
INITIAL DISTRIBUTION LIST.....		49

ACKNOWLEDGMENT

I would like to thank Professor Powers and Professor Ha for their guidance, support and encouragement. I would also like to thank the staff and faculty of the Electrical Engineering department for their professionalism and support. Finally I would like to thank my family, my husband for his endless words of encouragement and support, my children for accepting and understanding my frequent absences and my parents who always believed in me.

I. INTRODUCTION

The Navy has taken an interest in fiber optic communications for several reasons. Fiber is considerably thinner and lighter than the traditional coaxial and twisted pair mediums used for communications which makes it easy to transport and easy to install within the small compartments on ships. In addition fiber is a noise-free medium that provides a wide bandwidth with increased communication security. Specifically, in regards to security, fiber is very difficult to tap because it is not electrical and does not radiate. The fact that it does not radiate makes it the cable of choice for classified communication circuits where TEMPEST must be maintained. Other favorable characteristics of fiber for military applications include its immunity to electromagnetic interference (EMI) and resistance to hazards. Fiber is more reliable than other media and continues to operate when subjected to wet areas, areas of high voltage and areas of frequent power surges. [Ref. 1]

At the Naval Postgraduate School (NPS) we are currently researching the potential for and feasibility of an optical signal demultiplexer based on the Mach-Zehnder coupler as shown in Figure 1.1. This thesis is a first step in that analysis and focuses on a single Mach-Zehnder coupler operating at 100 Mbps.

The Mach-Zehnder coupler shown in Figure 1.1 is composed of two 2x2 optical couplers, a delay element and a phase shift element. The signal that enters the first coupler (port 1) is divided and the output is sent through the two output ports (ports A and B). The signal that leaves port A is sent through a delay before it arrives at the second 2x2 coupler. The signal from port B has no added delay. At the second 2x2

coupler the signals are combined, equally divided and sent out through ports A and B. The output from port B of the second 2x2 coupler is then shifted in phase by ninety degrees.

By cascading a number of Mach-Zehnder couplers together that are slightly different from one another (i.e., they have different delays), we would be able to discriminate between different code shift keying (CSK) signals. (Code shift keying is obtained by varying the phase of a sinusoidal carrier between 0 and π radians.) For example, suppose we would like to build a filter that was capable of isolating two CSK signals. Figure 1.2 shows a two-stage Mach-Zehnder demultiplexer capable of discriminating between four CSK signals. The four CSK signals are encoded by four Hadamard codes [Ref. 2]. The first Mach-Zehnder coupler combines the energy in the first two CSK pulses and the second Mach-Zehnder couplers combine the energy in all the CSK pulses. The results of the second Mach-Zehnder couplers are sent to photodetectors which convert the optical signal to electrical and then integrate it over a one pulse duration. This example can be expanded to include n Mach-Zehnder stages where $n = \log_2 M$ ($M = 2^n$). Each stage would have a different delay, capable of discriminating between M different CSK signals employing M Hadamard codes. [Ref. 3]

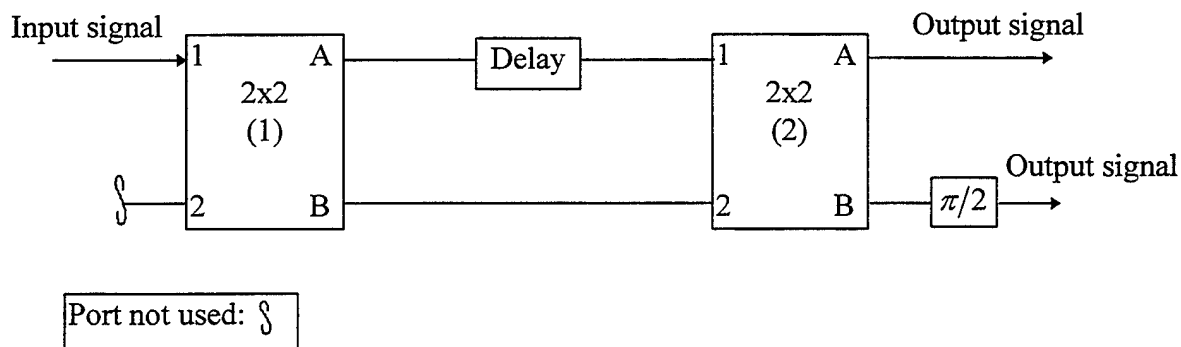


Figure 1.1 The Mach-Zehnder coupler.

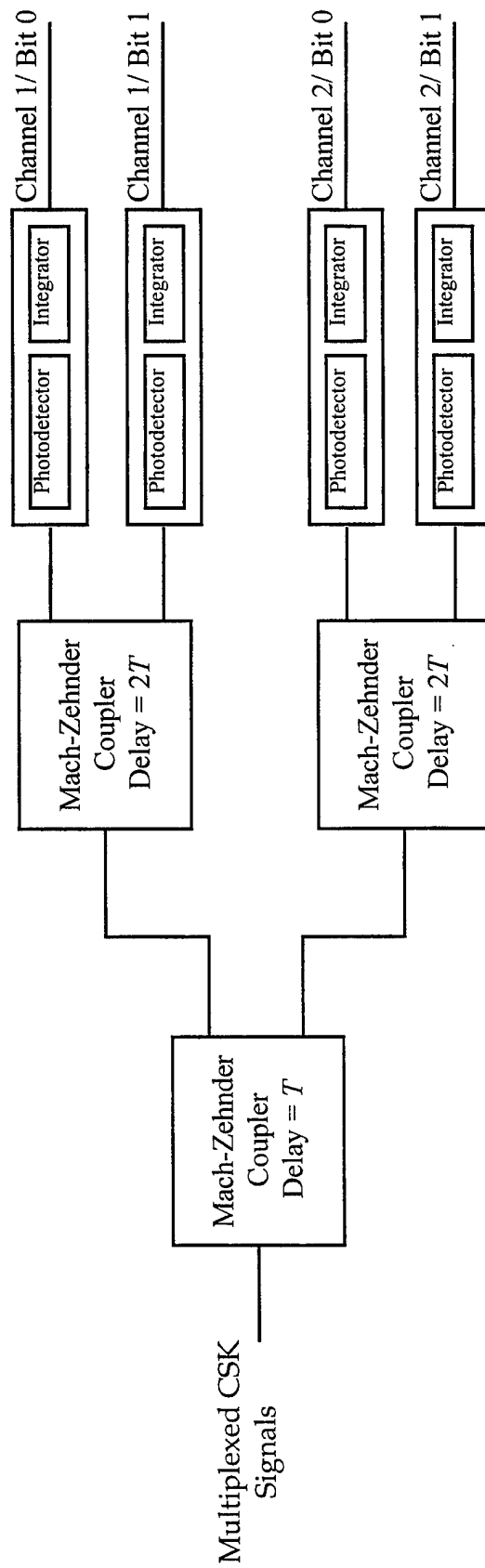


Figure 1.2 Block diagram of a two stage Mach-Zehnder demultiplexer.

In the second chapter of this thesis we develop and discuss the theory behind the Mach-Zehnder coupler. The chapter also includes an analysis of a signal in both the time and frequency domains as it transits the Mach-Zehnder coupler. Chapter III focuses on the actual building and testing of the Mach-Zehnder coupler. Each component of the coupler will be examined and measured to determine the placement of individual components in order to create the most successful Mach-Zehnder coupler. In addition, Chapter III discusses the equipment used to both run and test the Mach-Zehnder coupler. In Chapter IV the thesis concludes with a discussion of the performance of the Mach-Zehnder coupler, identification of difficulties encountered while building the coupler and suggestions for improving its performance. Appendix A is a complete description of the equipment and procedure used to measure the insertion loss. Appendix B describes the method and equipment used to measure the time delay.

II. THE MACH-ZEHNDER COUPLER

A. OVERVIEW OF THE MACH-ZEHNDER COUPLER

In this chapter we describe the function of the Mach-Zehnder coupler shown in Figure 2.1. It consists of two 2x2 optical couplers, a delay line of T seconds (where T is one bit period of the digital data) and a $\pi/2$ phase shifter. Port 1 of the first coupler is the input. Port A of the second coupler and the output of the phase shifter are the two outputs. Let $s(t)$ be the equivalent lowpass signal of the input signal and $S(f)$ be its Fourier transform. The outputs, in the frequency domain, at ports A and B of the first 2x2 coupler will be shown to be $S(f)/\sqrt{2}$ and $jS(f)/\sqrt{2}$, respectively, where $j = \sqrt{-1}$. (Note that multiplication by j is equivalent to a $\pi/2$ phase shift.) The output of the delay line of T in the frequency domain is $(S(f)e^{-j2\pi f T})/\sqrt{2}$. The output, in the frequency domain, at port A of the second 2x2 coupler will be shown to be $(S(f)e^{-j2\pi f T} - S(f))/2$. The transform of the other output of the Mach-Zehnder coupler (i.e., the output of the $\pi/2$ phase shifter) will be $-(S(f)e^{-j2\pi f T} + S(f))/2$. In the time domain, the two outputs of the Mach-Zehnder coupler produced by the input signal $s(t)$ are $(s(t-T) - s(t))/2$ and $-(s(t-T) + s(t))/2$. Thus the Mach-Zehnder coupler produces outputs that are one half the differences of the input signal's delayed version and itself and an inverted representation of one-half the sum of the input and its delayed version.

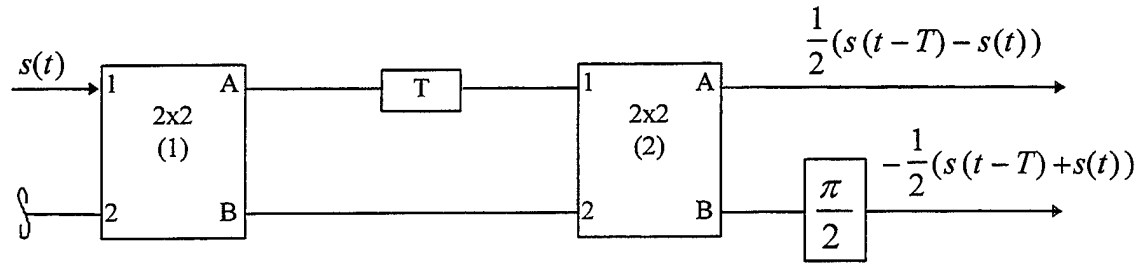


Figure 2.1 Block diagram of the Mach-Zehnder coupler.

B. ANALYTICAL DESCRIPTION OF COMPONENTS

In this section we mathematically analyze each component of the Mach-Zehnder coupler. The section concludes by tracing the signal as it transits through the complete Mach-Zehnder coupler.

1. 2x2 Coupler

The 2x2 coupler has four ports, identified in Figure 2.2 as 1, 2, A, and B. Each of these ports can be used as either an input or output.

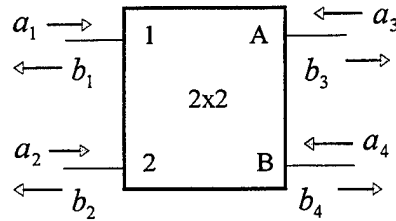


Figure 2.2 2x2 coupler.

Let the frequency domain inputs, \tilde{a}_i , and outputs, \tilde{b}_i (where \tilde{a}_i and \tilde{b}_i are the transforms of the signal a_i and b_i , respectively) of the 2x2 coupler shown in Figure 2.2 be described by the following vectors $\tilde{\mathbf{a}}$ and $\tilde{\mathbf{b}}$:

$$\tilde{\mathbf{a}} = \begin{bmatrix} \tilde{a}_1 \\ \tilde{a}_2 \\ \tilde{a}_3 \\ \tilde{a}_4 \end{bmatrix} \quad \tilde{\mathbf{b}} = \begin{bmatrix} \tilde{b}_1 \\ \tilde{b}_2 \\ \tilde{b}_3 \\ \tilde{b}_4 \end{bmatrix} \quad (2.1)$$

The input vector $\tilde{\mathbf{a}}$ and output vector $\tilde{\mathbf{b}}$ are related by the scattering matrix \mathbf{S} given by [Ref. 3]:

$$\mathbf{S} = \frac{1}{\sqrt{2}} \begin{bmatrix} 0 & 0 & 1 & j \\ 0 & 0 & j & 1 \\ 1 & j & 0 & 0 \\ j & 1 & 0 & 0 \end{bmatrix} \quad (2.2)$$

such that [Ref. 4]:

$$\tilde{\mathbf{b}} = \mathbf{S} \tilde{\mathbf{a}} \quad (2.3)$$

$$\begin{bmatrix} \tilde{b}_1 \\ \tilde{b}_2 \\ \tilde{b}_3 \\ \tilde{b}_4 \end{bmatrix} = \frac{1}{\sqrt{2}} \begin{bmatrix} 0 & 0 & 1 & j \\ 0 & 0 & j & 1 \\ 1 & j & 0 & 0 \\ j & 1 & 0 & 0 \end{bmatrix} \begin{bmatrix} \tilde{a}_1 \\ \tilde{a}_2 \\ \tilde{a}_3 \\ \tilde{a}_4 \end{bmatrix} \quad (2.4)$$

Equation 2.4 can be simplified by partitioning the matrix as shown below:

$$\begin{bmatrix} \tilde{b}_1 \\ \tilde{b}_2 \\ \tilde{b}_3 \\ \tilde{b}_4 \end{bmatrix} = \frac{1}{\sqrt{2}} \begin{bmatrix} 0 & 0 & 1 & j \\ 0 & 0 & j & 1 \\ 1 & j & 0 & 0 \\ j & 1 & 0 & 0 \end{bmatrix} \begin{bmatrix} \tilde{a}_1 \\ \tilde{a}_2 \\ \tilde{a}_3 \\ \tilde{a}_4 \end{bmatrix} \quad (2.5)$$

After partitioning, Equation 2.5 can be rewritten as:

$$\begin{bmatrix} \tilde{b}_1 \\ \tilde{b}_2 \end{bmatrix} = \frac{1}{\sqrt{2}} \begin{bmatrix} 1 & j \\ j & 1 \end{bmatrix} \begin{bmatrix} \tilde{a}_3 \\ \tilde{a}_4 \end{bmatrix} = \begin{bmatrix} (\tilde{a}_3 + j\tilde{a}_4)/\sqrt{2} \\ (j\tilde{a}_3 + \tilde{a}_4)/\sqrt{2} \end{bmatrix} \quad (2.6a)$$

$$\begin{bmatrix} \tilde{b}_3 \\ \tilde{b}_4 \end{bmatrix} = \frac{1}{\sqrt{2}} \begin{bmatrix} 1 & j \\ j & 1 \end{bmatrix} \begin{bmatrix} \tilde{a}_1 \\ \tilde{a}_2 \end{bmatrix} = \begin{bmatrix} (\tilde{a}_1 + j\tilde{a}_2)/\sqrt{2} \\ (j\tilde{a}_1 + \tilde{a}_2)/\sqrt{2} \end{bmatrix} \quad (2.6b)$$

We observe from partitioning and rewriting Equation 2.5 that (ideally) no part of the transform of the input signal is reflected back through the input ports. Specifically, in Equation 2.6(b) \tilde{b}_3 and \tilde{b}_4 are the only outputs when \tilde{a}_1 and \tilde{a}_2 are used as inputs. [Ref. 4]

Now consider the case shown in Figure 2.3 where \tilde{a}_1 is the transform of the input signal a_1 at port 1 and the second input at port 2 is not connected (i.e., $\tilde{a}_2 = 0$). Using Equation 2.6b:

$$\begin{bmatrix} \tilde{b}_3 \\ \tilde{b}_4 \end{bmatrix} = \begin{bmatrix} \tilde{a}_1/\sqrt{2} \\ j\tilde{a}_1/\sqrt{2} \end{bmatrix} \quad (2.7)$$

Hence, we see that the output amplitudes are decreased by a factor of $1/\sqrt{2}$ and that the second output is phase shifted by $\pi/2$ from the first output.

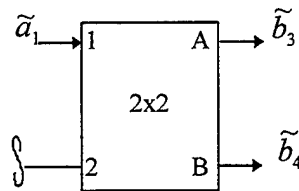


Figure 2.3 2x2 coupler with only one input port connected.

2. Delay Line

As shown in Figure 2.4, the signal is delayed by a period of T as it passes through the delay. If the transform of the input signal is \tilde{a}_1 , then the output after passing through the delay will be $\tilde{a}_1 e^{j2\pi T}$ in the frequency domain.

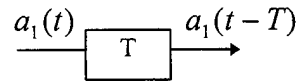


Figure 2.4 Time delay.

3. Phase Shifter

As shown in Figure 2.5, as the transform of the signal passes through the $\pi/2$ phase shifter, it is multiplied by j ($= e^{j\pi/2}$).

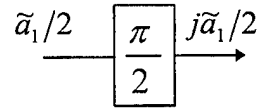


Figure 2.5 Phase shifter.

C. SIGNAL ANALYSIS OF THE MACH-ZEHNDER COUPLER

Using the preceding analysis we now completely describe the Mach-Zehnder coupler, Figure 2.6, in the time and frequency domain. Let $s(t)$ be the equivalent

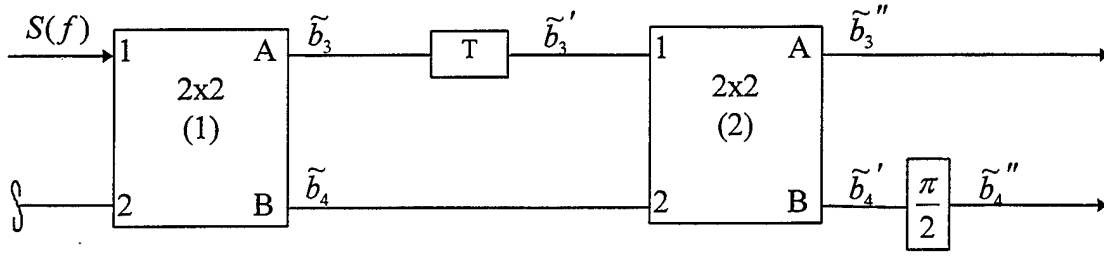


Figure 2.6 Mach-Zehnder coupler.

lowpass signal of the input signal and $S(f)$ be its Fourier transform. Using Equation 2.7 for a 2x2 coupler with only one input, where $\tilde{a}_1 = S(f)$, we find the transform of output, \tilde{b}_3 and \tilde{b}_4 :

$$\begin{bmatrix} \tilde{b}_3 \\ \tilde{b}_4 \end{bmatrix} = \begin{bmatrix} S(f)/\sqrt{2} \\ jS(f)/\sqrt{2} \end{bmatrix} \quad (2.8)$$

Prior to arriving at the second 2x2 coupler, \tilde{b}_3 will pass through a delay. A delay of T in the time domain results in a multiplication by a $e^{j2\pi f T}$ in the frequency domain. Letting \tilde{b}_3' represent \tilde{b}_3 after it passes through the delay, then the inputs to the second 2x2 coupler can be written as:

$$\begin{bmatrix} \tilde{b}_3' \\ \tilde{b}_4 \end{bmatrix} = \begin{bmatrix} e^{-j2\pi f T} & 0 \\ 0 & 1 \end{bmatrix} \begin{bmatrix} S(f)/\sqrt{2} \\ jS(f)/\sqrt{2} \end{bmatrix} = \begin{bmatrix} S(f)e^{-j2\pi f T}/\sqrt{2} \\ jS(f)/\sqrt{2} \end{bmatrix} \quad (2.9)$$

The transform of the outputs of the second coupler, \tilde{b}_3'' and \tilde{b}_4' , are found by using Equation 2.6b with \tilde{b}_3' and \tilde{b}_4 as the input (i.e., in Equation 2.6(b) let $\tilde{a}_1 = \tilde{b}_3'$ and $\tilde{a}_2 = \tilde{b}_4$).

$$\begin{bmatrix} \tilde{b}_3'' \\ \tilde{b}_4' \end{bmatrix} = \frac{1}{\sqrt{2}} \begin{bmatrix} 1 & j \\ j & 1 \end{bmatrix} \begin{bmatrix} S(f)e^{-j2\pi f T}/\sqrt{2} \\ jS(f)/\sqrt{2} \end{bmatrix} = \begin{bmatrix} (S(f)e^{-j2\pi f T} - S(f))/2 \\ j(S(f)e^{-j2\pi f T} + S(f))/2 \end{bmatrix} \quad (2.10)$$

The final output of the Mach-Zehnder coupler, \tilde{b}_3'' and \tilde{b}_4'' is seen after \tilde{b}_4' passes through the ninety degree phase shifter.

$$\begin{bmatrix} \tilde{b}_3'' \\ \tilde{b}_4'' \end{bmatrix} = \begin{bmatrix} 1 & 0 \\ 0 & j \end{bmatrix} \begin{bmatrix} (S(f)e^{-j2\pi f T} - S(f))/2 \\ j(S(f)e^{-j2\pi f T} + S(f))/2 \end{bmatrix} = \begin{bmatrix} (S(f)e^{-j2\pi f T} - S(f))/2 \\ -(S(f)e^{-j2\pi f T} + S(f))/2 \end{bmatrix} \quad (2.11)$$

By taking the inverse Fourier transform of Equation 2.11, we can see the output signals b_3'' and b_4'' in the time domain are:

$$\begin{bmatrix} b_3'' \\ b_4'' \end{bmatrix} = \begin{bmatrix} (s(t-T) - s(t))/2 \\ -(s(t-T) + s(t))/2 \end{bmatrix} \quad (2.12)$$

By multiplying the matrices used to represent the phase shift, delay and two couplers (Equation 2.13), we can derive a general equation (Equation 2.14(a), 2.14(b)) where the output of the Mach-Zehnder coupler can be readily determined from the inputs \tilde{a}_1 and \tilde{a}_2 .

$$\begin{bmatrix} \tilde{b}_3'' \\ \tilde{b}_4'' \end{bmatrix} = \underbrace{\begin{bmatrix} 1 & 0 \\ 0 & j \end{bmatrix}}_{\text{Phase shift}} \underbrace{\frac{1}{\sqrt{2}} \begin{bmatrix} 1 & j \\ j & 1 \end{bmatrix}}_{\text{2nd Coupler}} \underbrace{\begin{bmatrix} e^{-j2\pi fT} & 0 \\ 0 & 1 \end{bmatrix}}_{\text{Delay}} \underbrace{\frac{1}{\sqrt{2}} \begin{bmatrix} 1 & j \\ j & 1 \end{bmatrix}}_{\text{1st Coupler}} \begin{bmatrix} \tilde{a}_1 \\ \tilde{a}_2 \end{bmatrix} \quad (2.13)$$

$$\begin{bmatrix} \tilde{b}_3'' \\ \tilde{b}_4'' \end{bmatrix} = \frac{1}{2} \begin{bmatrix} (e^{-j2\pi fT} - 1) & (je^{-j2\pi fT} + j) \\ (-e^{-j2\pi fT} - 1) & (-je^{-j2\pi fT} + j) \end{bmatrix} \begin{bmatrix} \tilde{a}_1 \\ \tilde{a}_2 \end{bmatrix} \quad (2.14a)$$

$$\begin{bmatrix} \tilde{b}_3'' \\ \tilde{b}_4'' \end{bmatrix} = \frac{1}{2} \begin{bmatrix} \tilde{a}_1(e^{-j2\pi fT} - 1) + \tilde{a}_2j(e^{-j2\pi fT} + 1) \\ \tilde{a}_1(-e^{-j2\pi fT} - 1) - \tilde{a}_2j(e^{-j2\pi fT} - 1) \end{bmatrix} \quad (2.14b)$$

D. SUMMARY

In this chapter we learned that the 2x2 coupler combines the signals from its two input ports, splits the signal and sends the result through the two output ports, and that both output signals leave the coupler simultaneously. We also determined that, if only one input port is used, then no part of the input signal is reflected back through the second input port. We have also seen that the outputs from the Mach-Zehnder coupler are $(S(f)e^{-j2\pi fT} - S(f))/2$ and $-(S(f)e^{-j2\pi fT} + S(f))/2$ in the frequency domain or, equivalently, $(s(t - T) - s(t))/2$ and $-(s(t - T) + s(t))/2$ in the time domain.

In the next chapter we will discuss the actual building and testing of the Mach-Zehnder coupler. Specifically we will look at each component of the Mach-Zehnder coupler and measure its insertion loss as well as any delay that it imposes on the signal.

This information will be used to determine the placement of individual components in order to create the most successful Mach-Zehnder coupler. In addition Chapter III discusses the equipment used to both run and test the coupler. The chapter concludes by showing the arrangement and performance of two different configurations of the Mach-Zehnder coupler.

III. HARDWARE DESCRIPTION

In this chapter we discuss the hardware used to build a Mach-Zehnder coupler (Figure 3.1) that will operate with a digital optical signal at 100 Mbps and have a one bit period delay. Notice that Figure 3.1 introduces a third 2x2 coupler; we will see later in this chapter that the additional coupler is used to provide the required $\pi/2$ phase shift. The nature of this experiment requires knowledge of each component's individual characteristics, specifically the insertion loss and timing delay that each device imposes on the system. This chapter will discuss all of the components in detail and include results of necessary measurements as well as documenting the method used to determine such losses and delays.

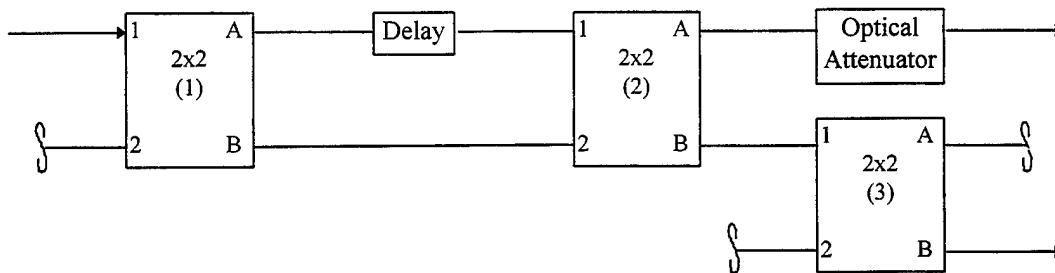


Figure 3.1 Mach-Zehnder coupler.

A. 2x2 COUPLER

All of the couplers used in this experiment were single mode and manufactured by Fiber Institute Sales Inc. (model number F193205). The couplers came equipped with pigtails of one meter length, terminated with ST connectors.

1. Insertion Loss

Since this experiment involves transmitting a signal through various fiber optic components, the power loss of each coupler must be determined in order to establish which arrangement of available components will provide the least combined loss. Figure 3.2 illustrates the setup used to measure the power losses of the 2x2 couplers. The diode laser controller, shown in Figure 3.2, is computer controlled, allowing the user to select the mode of operation (power or current) and then to digitally specify the operating temperature and power (or current) requirements [Ref. 5]. For this experiment, the controller was set in the power mode, at 0.17 mW at a temperature of 10C. (The value of input power used was chosen arbitrarily based a 1 mW maximum input power for the diode in addition to the input power limitations of the devices under test.) The controller was connected to a 1300 nm laser diode. The optical output of the laser diode was transmitted through a one meter length of single mode fiber which was connected to the input port of the 2x2 coupler (port 1, Figure 3.2). The output of the 2x2 coupler (port A of Figure 3.2) was sent to the optical multimeter, which was equipped with a Power/WaveHead. The Power/WaveHead was designed to simultaneously measure

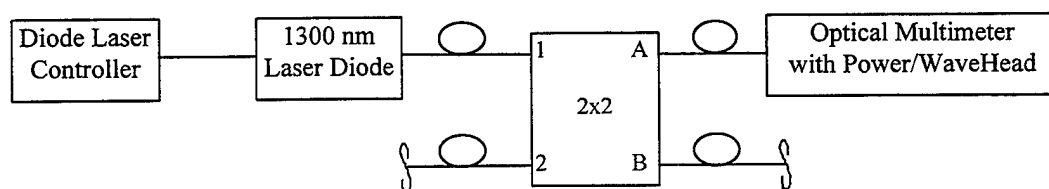


Figure 3.2 Block diagram of the procedure used to measure insertion losses of the 2x2 coupler.

power and wavelength from the laser source, thereby enabling it to automatically calibrate the wavelength-dependent response of its InGaAs detector. The optical multimeter provides a six-digit display with a linear power range of 0.000 nW to 999.999 W. The multimeter accepted wavelengths from 1040 to 1600 nm and accurately measured power to within $\pm 3.5\%$ and wavelength to within ± 1 nm [Ref. 6].

Prior to each test the output of the laser diode was connected directly to the input of the optical multimeter (Figure 3.3). This reading was recorded as the input power to the system. Once the input power was determined, the 2x2 was inserted between the laser diode and the optical multimeter as shown in Figure 3.2. The reading from the optical multimeter was recorded as the output power. Both the input and output power were rounded to the nearest 0.01 μW . The loss was computed as the ratio of input power to the output power, with the result converted to decibels. For a more detailed description of the equipment and procedure used to measure the insertion losses, see Appendix A.

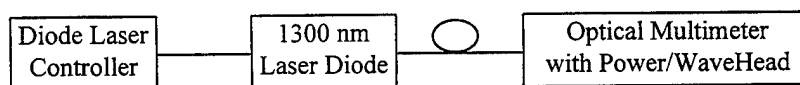
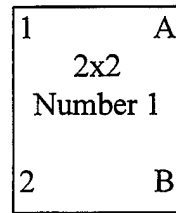


Figure 3.3 Block diagram illustrating setup used to measure input power.

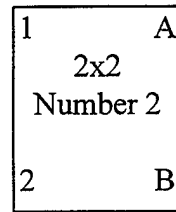
Figure 3.4 provides the recorded insertion losses for all three couplers used in this experiment and reflects information gathered when each of the four ports of the 2x2 coupler was used as an input port. For example in Figure 3.4(a) when port 1 of 2x2 number 1 was used as the input port, the recorded losses at output ports A and B

Input		Output	
		A	B
1	1	4.33	4.97
	2	5.59	4.21



(a)

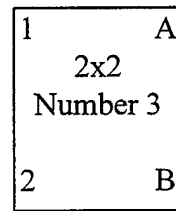
Input		Output	
		1	2
A	1	4.01	5.03
	2	4.92	4.34



(b)

Input		Output	
		A	B
1	1	4.00	3.51
	2	4.06	4.23

Input		Output	
		1	2
A	1	5.83	5.35
	2	3.90	6.12



(c)

Input		Output	
		A	B
1	1	4.26	7.59
	2	3.61	7.72

Input		Output	
		1	2
A	1	4.56	4.65
	2	7.28	7.61

Figure 3.4 Insertion losses measured in dB for (a) 2x2 coupler number 1, (b) 2x2 coupler number 2, (c) 2x2 coupler number 3.

were 4.33 dB and 4.97 dB, respectively. According to the specification sheet, 3.8 dB is a typical insertion loss. Our measured power losses varied from a low of 3.51 dB (seen in Figure 3.4(b) when port 1 of the number 2 2x2 was used as an input and port B was used as the output port) to a maximum loss of 7.72 dB (seen in Figure 3.4(c) when port 2 of the number 3 2x2 coupler was used as an input and the output was taken at port B).

2. Time Delay

In addition to the insertion losses added by the couplers, we are also interested in any differential time delay that a signal may exhibit at the two outputs of the coupler.

Since this experiment involves delaying one signal by one bit period relative to the other after they exit the first 2x2, we need ensure that the input signal exits the two output ports simultaneously. If one output signal should lead or lag the other, then that information would be needed in order to determine the amount of additional delay required to put the two output signals out of synchronization by one bit period at the input to the second coupler as required by the Mach-Zehnder coupler's specifications.

Figure 3.5 shows the experimental setup that was used to measure any time delay between the outputs of the couplers. The pattern generator, shown in Figure 3.5, produces a random sequence or user-programmed pattern with a data rate up to 3 Gbps [Ref. 7].

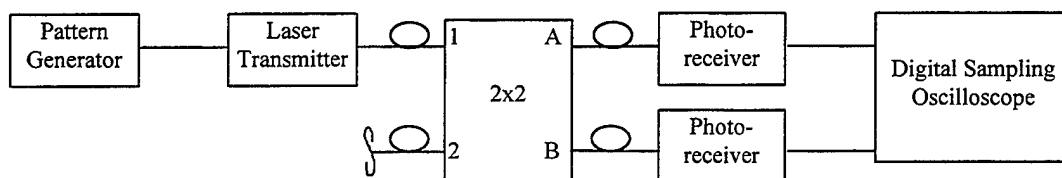
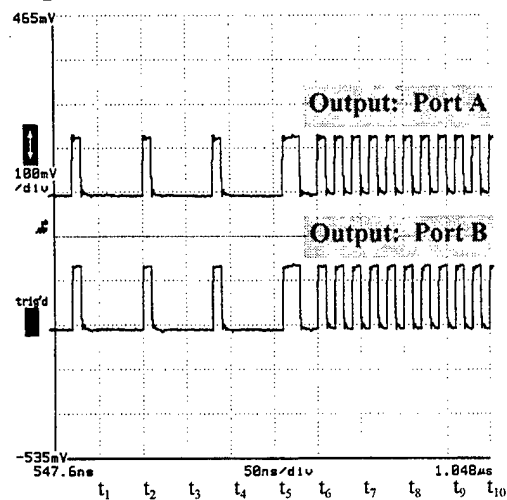


Figure 3.5 Block diagram of procedure used to measure time delay.

We programmed it to produce a repeating pattern at 100 Mbps. The electrical output of the generator is sent to the laser transmitter which is capable of accepting digital signals up to 1.3 Gbps and then transmitting a modulated 1300 nm optical signal [Ref. 8]. The output of the transmitter was connected to the input port of the 2x2 coupler under test (port 1 of Figure 3.5); each of the two output ports (ports A and B of Figure 3.5) was then connected to a photoreceiver. Each photoreceiver was an InGaAs PIN photodiode followed by a low-noise amplifier [Ref. 9]. The electrical output of the photoreceivers is sent to the digital sampling oscilloscope, which had a time measurement level accuracy of ± 4 ps. The oscilloscope is equipped with a SD-14 sampling head which provides dual-channel, 3 GHz sampling probes [Ref. 9]. For a more detailed description of the procedure and equipment used to measure the signal delay, see Appendix B.

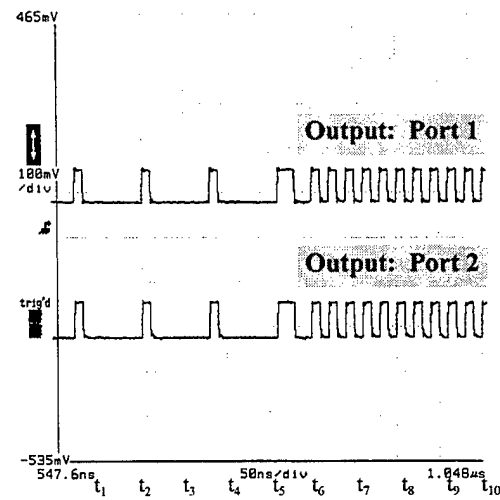
Figures 3.6, 3.7 and 3.8 contain the oscilloscope printouts and provide the required timing information for the three couplers. In Figure 3.6(a) we note that port 1 of 2x2 number 1 was used as the input port and the printout shows the envelope of the output signals seen at port A (top) and port B (bottom). (We will call these digital envelopes of the optical signals, the “digital signals”.) The vertical axis of the graph measures voltage with 100 mV per division. The horizontal axis is time with 50 ns per

Input: Port 1



(a)

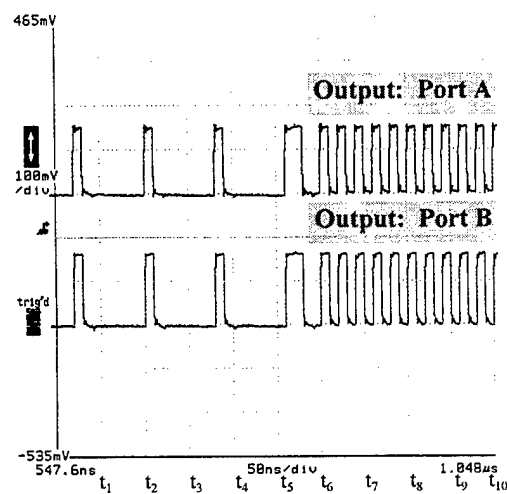
Input: Port A



(b)

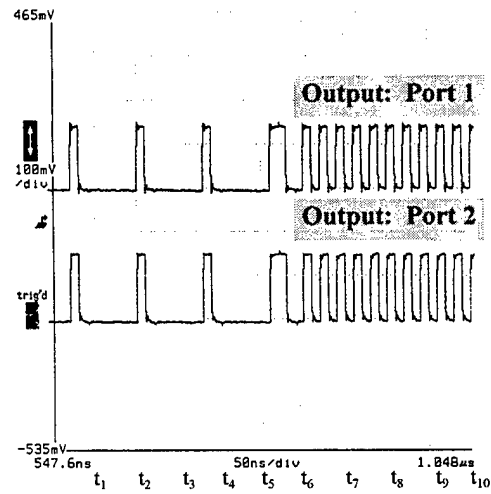
1	A
2x2	
Number	
1	
2	B

Input: Port 2



(c)

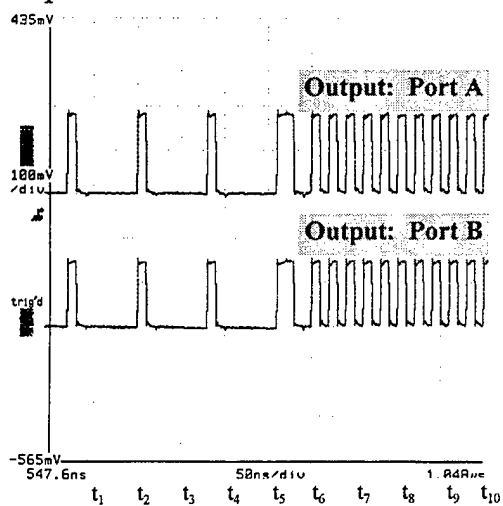
Input: Port B



(d)

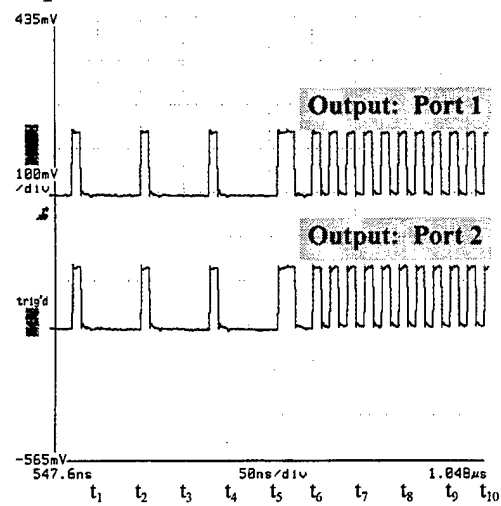
Figure 3.6 Timing delay for 2x2 coupler number 1 when each of the four ports is used as the input port. (a) Port 1 is the input port. (b) Port A is the input port. (c) Port 2 is the input port. (d) Port B is the input.

Input: Port 1



(a)

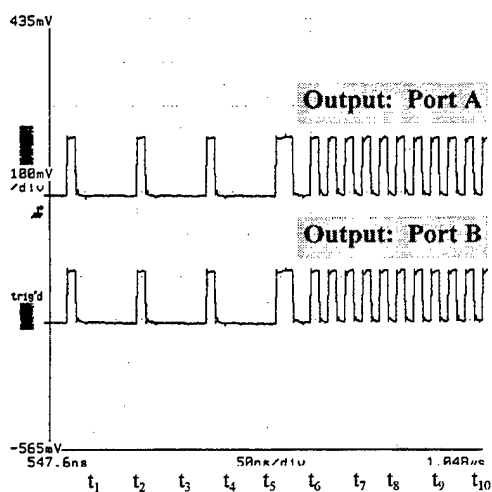
Input: Port A



(b)

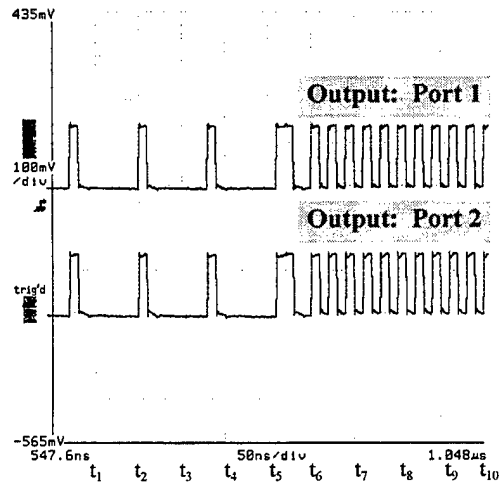
1	A
2x2	
Number	
2	
2	B

Input: Port 2



(c)

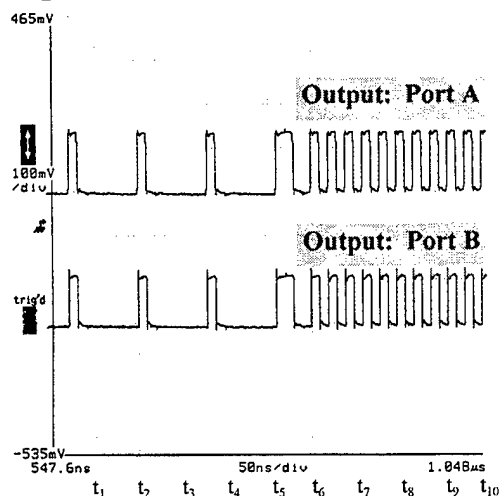
Input: Port B



(d)

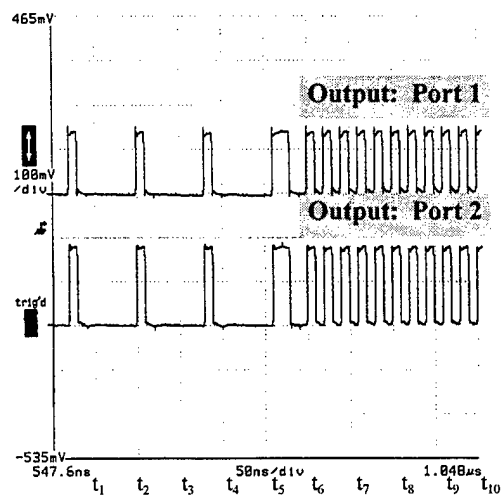
Figure 3.7 Timing delay for 2x2 coupler number 2 when each of the four ports is used as the input port. (a) Port 1 is the input port. (b) Port A is the input port. (c) Port 2 is the input port. (d) Port B is the input.

Input: Port 1



(a)

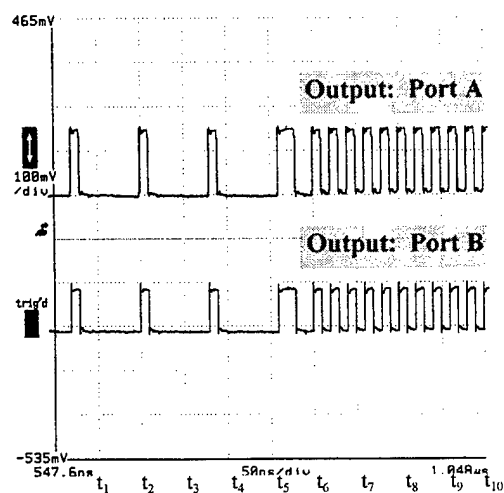
Input: Port A



(b)

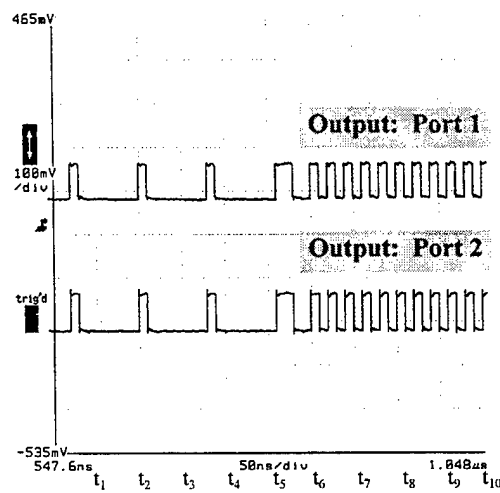
1	A
2x2	
Number	
3	
2	B

Input: Port 2



(c)

Input: Port B



(d)

Figure 3.8 Timing delay for 2x2 coupler number 3 when each of the four ports is used as the input port. (a) Port 1 is the input port. (b) Port A is the input port. (c) Port 2 is the input port. (d) Port B is the input.

division. When we compare the two digital signals, we note that they are in synchronization with one another, with no delay for one digital signal relative to the other. From studying the output digital signals of all three couplers we note that, while some of the paired digital signals may differ slightly in amplitude (as seen in Figure 3.8 (c)), all of the output digital signals leave the 2x2 couplers at the same time with no apparent additional delay experienced by one port with respect to another.

B. DELAY LINE

In order to create the required one bit-period delay, an extra length of fiber was inserted between the first and second coupler, as shown in Figure 3.9. The fiber used was 9/125 single mode fiber with single mode 127 μm ST connectors at each end.

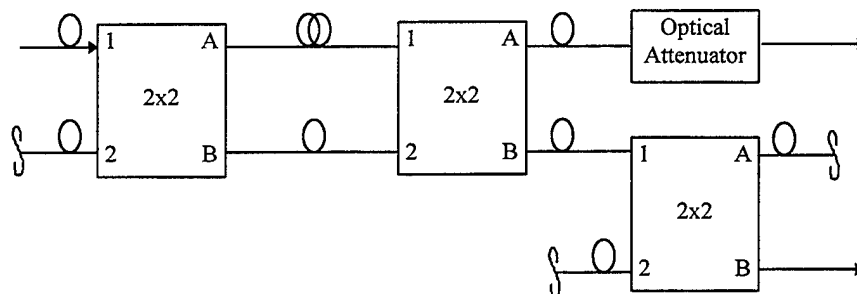


Figure 3.9 Block diagram showing additional length of fiber added between the first and second coupler.

1. Fiber Length

The length of fiber needed to create a T_b second delay is given by:

$$L = \frac{c}{1.45} T_b \quad (3.1)$$

where L is the length in meters, c is the speed of light, 1.45 is the index of refraction for light in the glass and T_b is the bit period. Our data rate was be 100 Mbps; therefore the bit period (T_b) was be 10 ns. Solving Equation 3.1 for L we find:

$$L = \frac{3.0 \times 10^8}{1.45} (1 \times 10^{-8}) = 2.07 \text{ m} \quad (3.2)$$

A single-mode fiber cable was cut to this length and single-mode ST connectors were added to each end.

2. Insertion Loss

The insertion loss of the fiber and its connectors was determined by using the arrangement shown in Figure 3.10. This is the same setup described earlier for measuring the insertion loss of the 2x2 coupler. Prior to inserting the delay fiber, the laser diode output pigtail was connected directly to the optical multimeter. This reading is recorded as the input power. Once the measurement was complete, the delay fiber was inserted between the laser diode pigtail and the optical multimeter as shown in Figure 3.10. The power of output signal was then recorded from the optical multimeter. The loss was computed as the ratio of input power to the output power, with the result converted to decibels. The fiber optic cable tested measured 2.08 meters with a fiber and connector pair loss of 0.7 dB. (The fiber loss was negligible for this short length.)

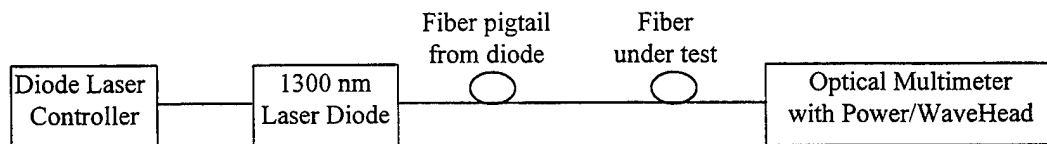


Figure 3.10 Block diagram illustrating procedure used to measure losses in fiber optic delay line.

3. Time Delay

The time delay was tested (Figure 3.11) by connecting the laser transmitter to input port 1 of a 2x2 coupler. The extra length of fiber was then connected to the coupler's output, port A, with the free end of the fiber connected to the photoreceiver. The output of port B was connected to a separate photoreceiver and the two digital signals were viewed on the oscilloscope. The time delay was measured using the oscilloscope's vertical bar cursors. For a more detailed description of the procedure and equipment used to measure the signal delay, see Appendix B.

Careful examination of the digital signal, Figure 3.12(a), at time t_2 confirms that output 1 lags output 2 by one bit period and 3.12(b) confirms a delay of 10 ns, as expected.

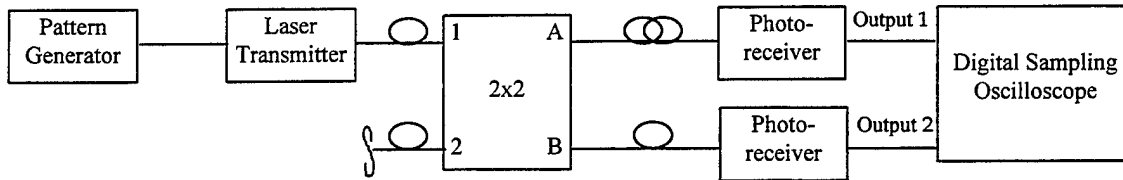


Figure 3.11 Block diagram of procedure used to measure bit period delay.

C. $\pi/2$ PHASE SHIFTER

We learned from Equation 2.7 that, if only one input port is used on a 2x2 coupler, then the transform of the two output signals will be $\tilde{a}_1/\sqrt{2}$ and $j\tilde{a}_1/\sqrt{2}$. From studying this, we note that both outputs are attenuated and one is ninety degrees out of

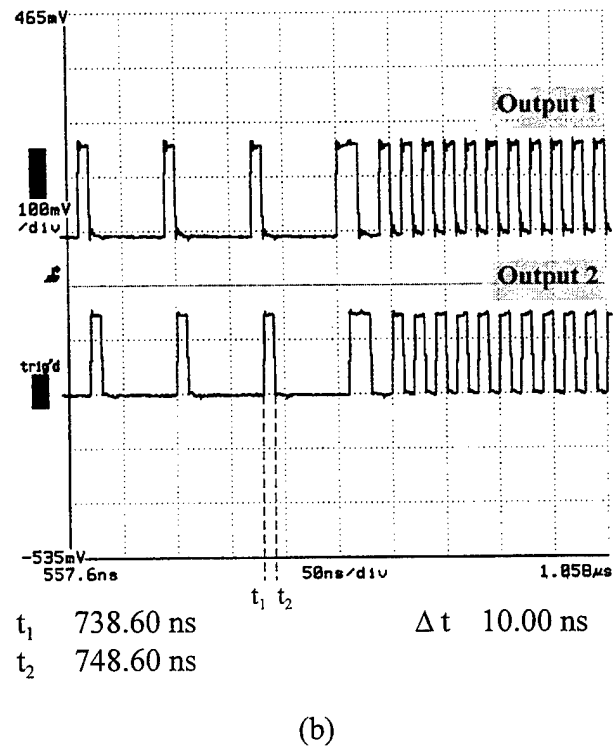
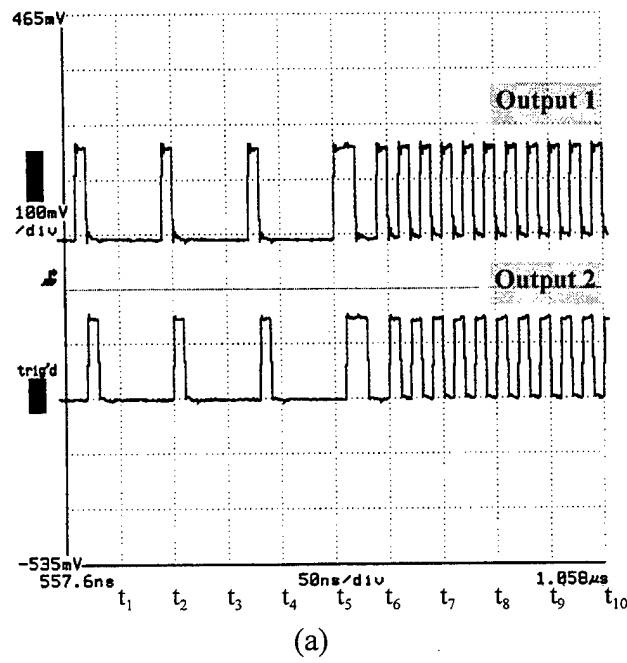


Figure 3.12 Delay created by inserting fiber between the first and second coupler:
 (a) shows delay and (b) shows that delay is 10 ns.

phase with \tilde{a}_1 , the transform of the input signal. Using this characteristic we can insert a third 2x2 coupler (Figure 3.13) to create the required $\pi/2$ radian phase shift. The additional 2x2 coupler reduces the signal power (output 2) that passes through it by at least 3 dB. In order to keep the two outputs of the Mach-Zehnder coupler at the same signal strength, the signal at output 1 is passed through an optical attenuator which provides a loss equal to the third 2x2 coupler. The value of the phase shift could be confirmed by conducting an interference experiment; however, equipment was not available to conduct an interferometer test.

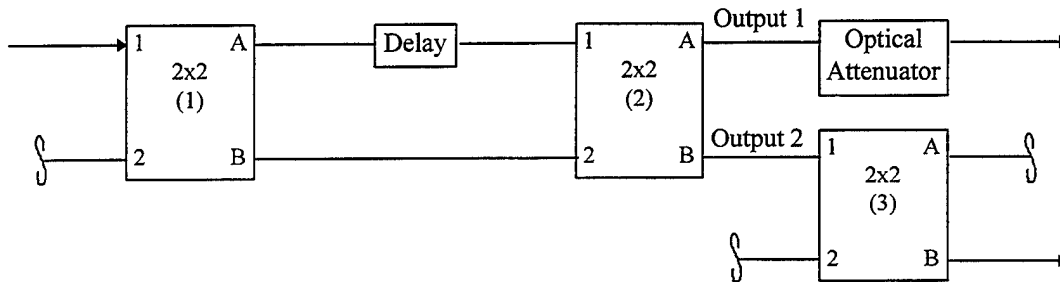


Figure 3.13. Block diagram of the Mach-Zehnder coupler showing the third 2x2 coupler used as a phase shifter.

D. ATTENUATOR

As previously stated, output 2 as seen in Figure 3.13, will experience at least a 3 dB loss as it passes through the 2x2 coupler which is used as a phase shifter. In order to keep the two output signals at the same power level, output 1 (Figure 3.13) was passed through an attenuator. The single-mode attenuator used for this experiment was manufactured by JDS Fitel (model number HA 9). The attenuator provided a digital display and was equipped with ST connectors.

1. Insertion Losses

The insertion loss of the attenuator used must not be greater than the expected 3 dB power loss of the 2x2 coupler. (Having an attenuator with a smaller insertion loss than the 2x2 coupler allows us to increase the attenuator's loss to match that of the 2x2 coupler.) Figure 3.14 illustrates the procedure that was used to measure the total loss of the attenuator. Prior to inserting the optical attenuator, the laser diode pigtail was connected directly to the optical multimeter and the reading from the optical multimeter was recorded as the input power. The optical attenuator was then inserted as shown in Figure 3.14. The loss was calculated as the ratio of the input power to the output power with the result converted to decibels. The attenuator was found to have an insertion loss of 2.02 dB when it was set to provide a loss of "0 dB" on the instrument's display panel. An additional 0.98 dB from the attenuator would give us our desired 3 dB (nominal) attenuation. See Appendix A for a more detailed description of the equipment and procedure used to measure the insertion losses.

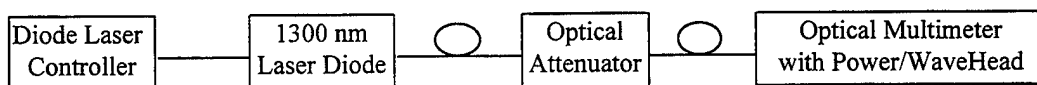


Figure 3.14 Block diagram illustrating procedure used to measure losses in optical attenuator.

E. THE MACH-ZEHNDER COUPLER

The equipment used in testing the Mach-Zehnder coupler is shown in Figure 3.15. The procedure used was the same described earlier to test for a signal delay in the 2x2 couplers. The pattern generator was configured to send a 100 Mbps repeating pattern to

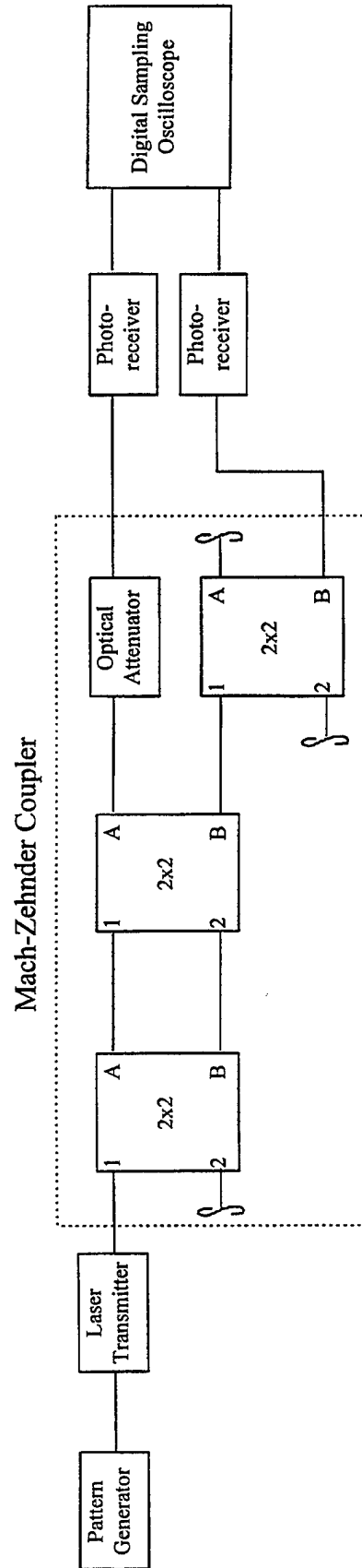


Figure 3.15 Block diagram showing complete setup .

the laser transmitter. The laser transmitter converted the signal from electrical to optical format, sending the optical signal to the input port of the Mach-Zehnder coupler. The output of the Mach-Zehnder was sent through two photoreceivers to the digital sampling oscilloscope. For a more detailed description of the procedure and equipment used to measure the performance of the Mach-Zehnder coupler, see Appendix B.

Using what we know about the components of the Mach-Zehnder coupler, we can now follow a digital signal as it transits through the Mach-Zehnder coupler and identify the changes that it undergoes. If the digital signal shown in Figure 3.16(a) is sent to the input port of the Mach-Zehnder coupler (port 1), the first 2x2 coupler will reduce the signal's amplitude by $1/\sqrt{2}$ and send it to the output ports A and B. The output digital signals from the first 2x2 coupler are shown in Figure 3.16(b). The signals are identified by coupler number and port (i.e., 1-A refers to coupler (1), port A, and 1-B is coupler (1), port B). We observe in Figure 3.16(b) that the two output digital signals have the same bit pattern as the input digital signal; however, their amplitude is reduced compared to the input digital signal. We also notice that the two digital output signals look identical to one another. This is to be expected since the digital signal representation does not include the optical carrier. If we could see the carrier, we would note that one carrier was ninety degrees out of phase with the other. Figure 3.16(c) shows the two signals as they enter the second 2x2 coupler. The top digital signal (2-1) is delayed by one bit period compared to the bottom digital signal (2-2) due to the delay fiber between the first and second couplers. At the second 2x2 coupler the digital signals are added (i.e., $0+1=1$, $1+1=2$, etc.) and then divided. Figure 3.16(d) show the output signals from by the second

Mach -Zehnder Coupler

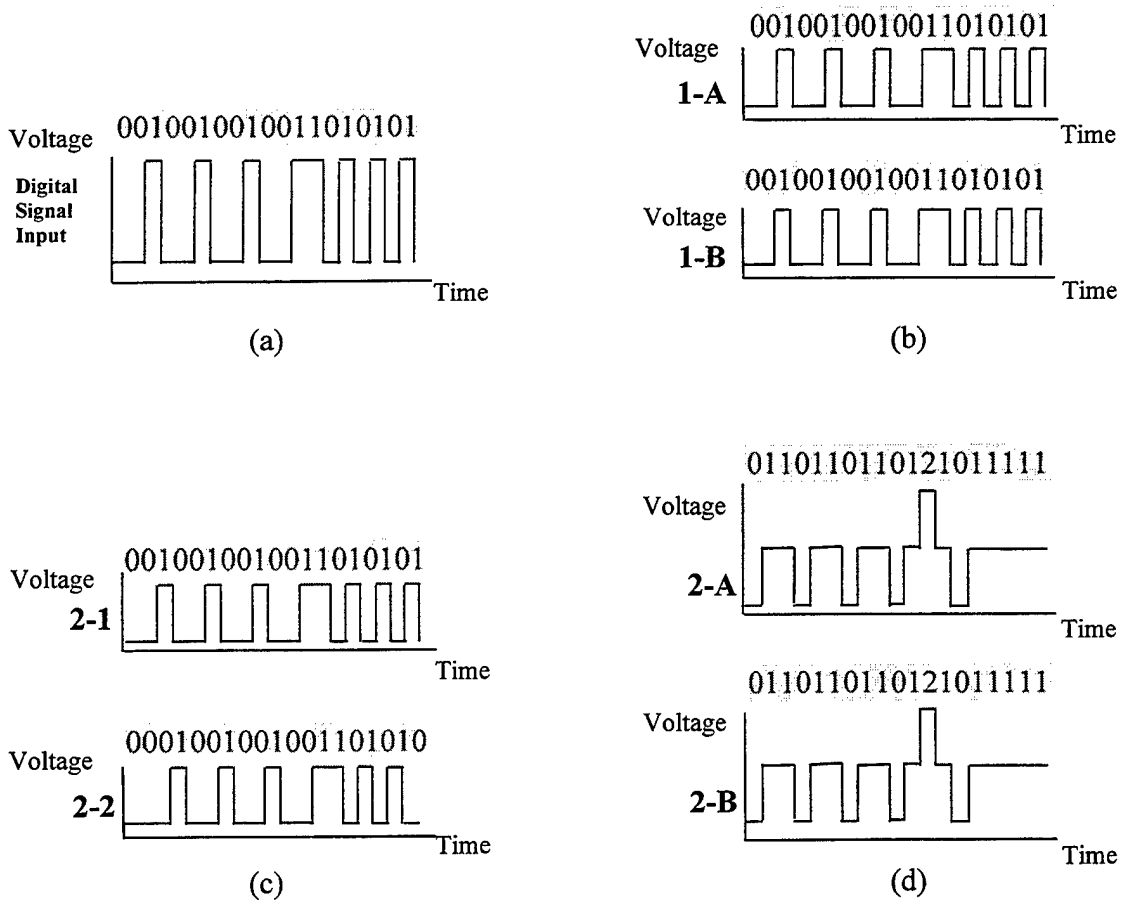
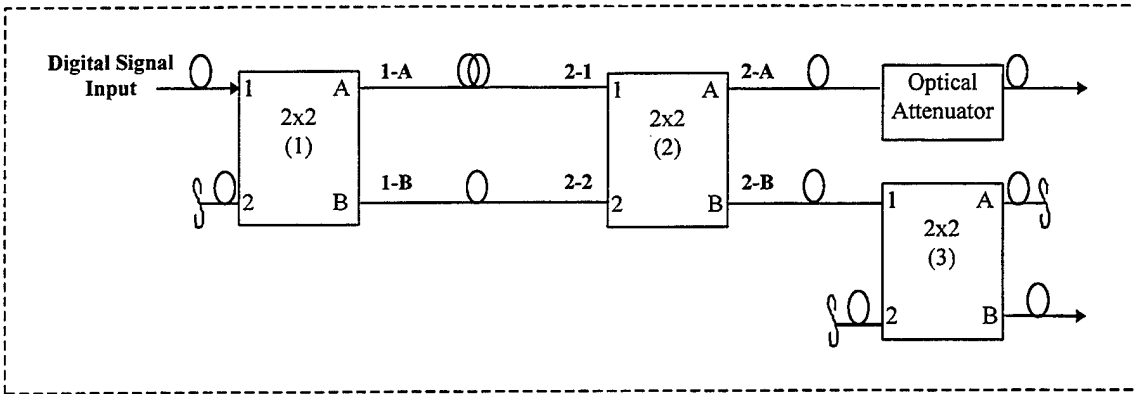
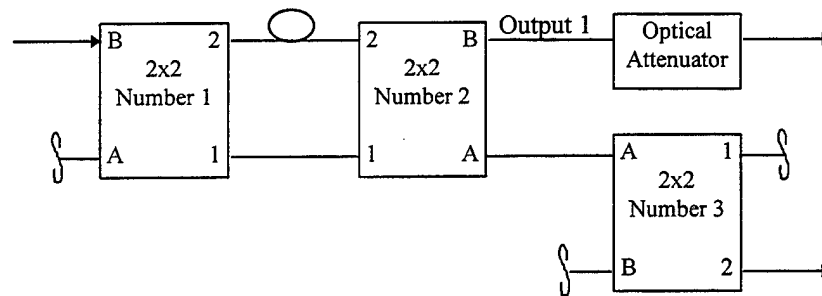


Figure 3.16 Qualitative description of the Mach-Zehnder coupler using the measured envelopes of the optical signal.

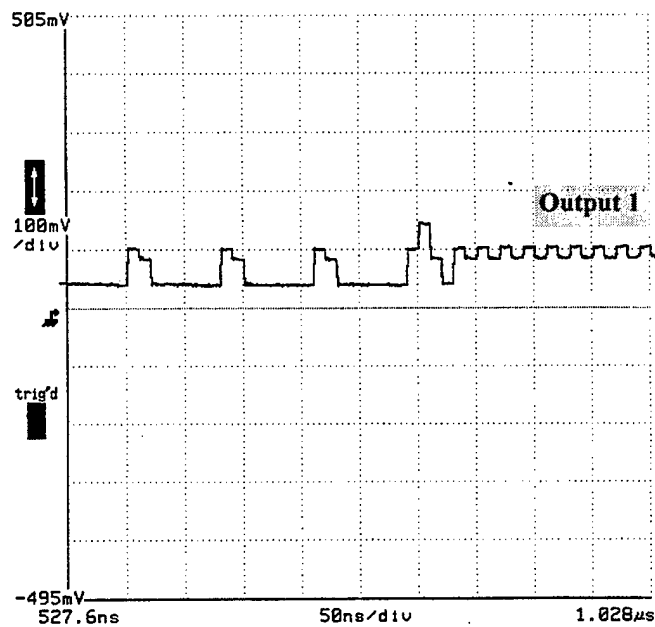
2x2 coupler. Notice that the two signals are again identical. This is due to the combining and dividing of the two signals by the coupler; while the inputs to the 2x2 coupler may be different, as was the case here, the output signals will always be identical. The signal at 2-A will be reduced in amplitude as it passes through the optical attenuator and the second signal (2-B) will be attenuated in power and phase shifted by ninety degrees as it passes through the third 2x2 coupler. The signal that appears at the attenuator output and at the output of the third coupler (3-B) will have the same pattern as shown in Figure 3.16(d) but with a smaller amplitude.

1. Setup

The first configuration which tested the placement of the components, couplers and the choice of ports used was based on creating the lowest overall insertion loss. Using the measured insertion losses (Figure 3.4), the components were distributed as shown in Figure 3.17(a) to achieve the lowest combined power loss. The setting of the attenuator was determined by subtracting the insertion loss of the attenuator from the insertion loss of the 2x2 coupler used as a phase shifter. In the case of this first configuration where port A of 2x2 number 3 is used as the input port of the phase-shifter and port 2 is the output port, the insertion loss (Figure 3.4(c)) is 4.65 dB. This requires that the attenuator be set at 2.43 dB ($4.45 \text{ dB} - 2.02 \text{ dB}$ (insertion loss of attenuator)). The digital signal sampled at the output of the second coupler (2x2 number 2) is shown in Figure 3.17(b). This digital signal, while similar to the expected output shown in Figure 3.16(d), does not maintain the voltage level between successive high voltage levels



(a)

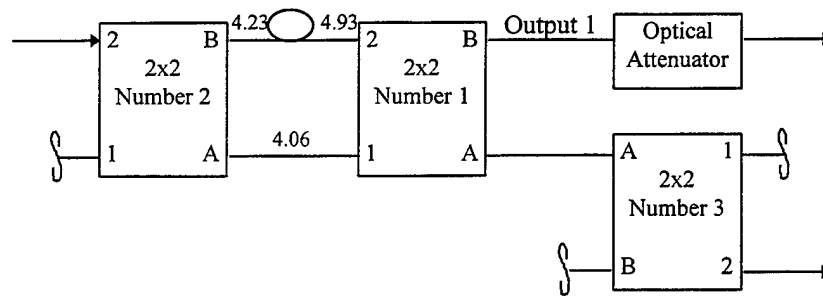


(b)

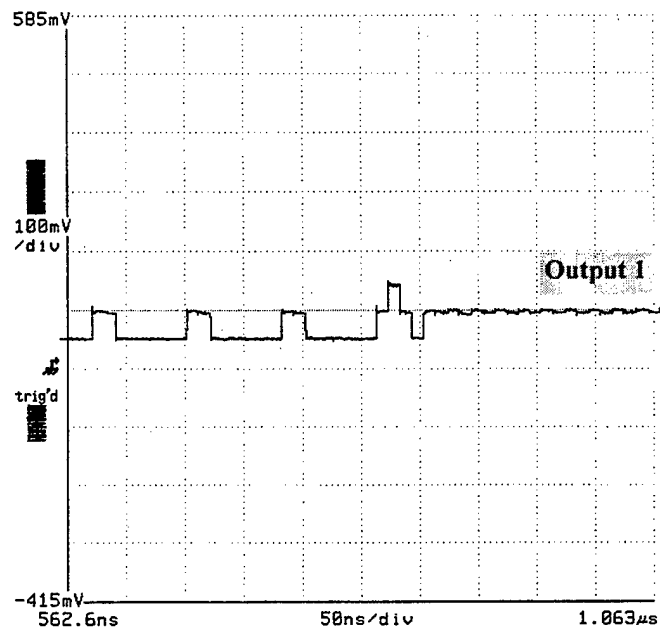
Figure 3.17 (a) Configuration based on lowest overall insertion loss. (b) Signal sampled at port B of second 2x2.

(bit 1). In addition, the end of the sample shows a fluctuation in voltage when it should be constant due to the high and low voltages continually adding to equal one as shown in Figure 3.16(d). These discrepancies could be due to either the digital signals that enter the second 2x2 coupler not being exactly one bit period out of phase with one another or the two digital signals experiencing a difference in power loss. Since we know that the extra length of fiber inserted created a one bit period delay (Figure 3.11) and all the 2x2 couplers output the signals simultaneously (Figures 3.6-3.8), the problem must result from a difference in power loss along the two signal paths. Using the information in Figure 3.4 and the measured insertion loss of the delay fiber and determine the total loss at port 2 of the second 2x2 as 5.73 dB ($5.03 \text{ dB} + 0.7 \text{ dB}$), and the loss at port 1 of 2x2 number 2 as 4.01 dB. This difference of 1.72 dB could account for the 20 mV drop in the amplitude of the digital signal shown in Figure 3.17(b).

Using the information in Figure 3.4, we reconfigured the system to provide a similar power loss at the input of the second 2x2 in the Mach-Zehnder coupler. The new arrangement is shown in Figure 3.18(a). Using the insertion loss data we calculate the loss of the two digital signals prior to entering the second coupler to be 4.93 dB at port 2 of the second 2x2 and 4.06 dB at port 1. The difference of 0.87 dB is almost half of the 1.72 dB seen in the first setup. The digital signal, sampled at the output of the second coupler (number 1), is shown in Figure 3.18(b). This digital signal, while still showing some voltage fluctuations, maps closer to the expected output shown in Figure 3.16(d).



(a)



(b)

Figure 3.18 (a) Configuration based on maintaining similar power loss. (b) Signal sampled at port B of second 2x2.

2. Results

Using the arrangement shown in Figure 3.18(a), the optical multimeter described earlier was used to record the power, measured in microwatts, at each connection in the Mach-Zehnder coupler. The results of these measurements are shown in Figure 3.19. Using the input power as a reference, the signal power loss, measured in dB, was recorded at each connection. The results of these measurements are seen in Figure 3.20. We see from the data in Figure 3.20 that this configuration results in an overall power loss of approximately 10.6 dB.

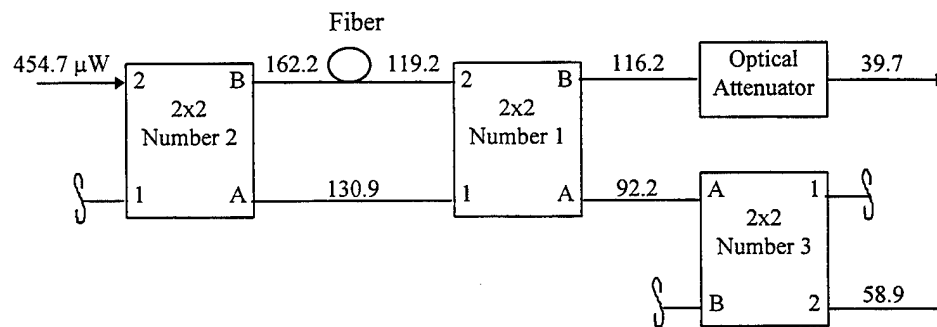


Figure 3.19 Signal power (in microwatts) measured at each connection.

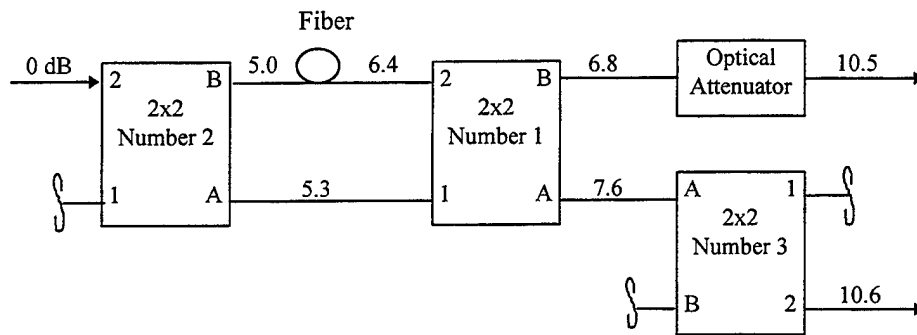


Figure 3.20 The signal loss (measured in dB) taken at each connection, with input power as the reference.

We have seen in this chapter that, by using the recorded insertion losses to choose the placement of each component, the signal quality can be greatly affected. We measured the signal loss of the last configuration to be 10.6 dB. This is a reasonable value considering that each of the three 2x2 couplers attenuated the signal power by a minimum of 3 dB.

In Chapter IV we will discuss the performance of the Mach-Zehnder coupler and identify difficulties encountered while building the coupler and suggestions for improving its performance.

IV. DISCUSSION AND CONCLUSIONS

Now that we have successfully built and tested the Mach-Zehnder coupler, we will discuss and identify difficulties encountered while building the coupler and present suggestions for improving its performance.

In Chapter III we determined that 207 cm was the optimum length of fiber required to create a one bit period delay at 100 Mbps. The actual length of fiber used was 208 cm. At the time of the experiment we did not specify a tolerance for the bit period delay. Our goal was to build a Mach-Zehnder coupler to exact specifications; however single mode fiber fractures easily due to the tighter tolerance of the single mode ferrule (i.e., ferrule tolerances are $+1/-0\text{ }\mu\text{m}$ for single mode connectors compared to $+2/-0\text{ }\mu\text{m}$ for multimode connectors). This tighter tolerance requires careful cleaning and insertion of the fiber. Failure to adequately clean the fiber will prevent the fiber from passing through the connector and lead to breakage [Ref. 11], thereby changing the overall fiber length. Creation of a length of fiber that is within one centimeter of a specified length of over two meters is considered very good. The additional one centimeter represented a 0.5% error with respect to the bit period. Had we built the same Mach-Zehnder coupler with a specified bit period delay tolerance of 2%, the required fiber length would be $207 \pm 4\text{ cm}$. From Equation 3.1 we know that the length of fiber used to create a one bit period delay is proportional to the bit period; as the bit period increases, so does the length of fiber required to create the delay. The bit period, however, is defined as the inverse of the data rate so that, as the data rate increases, the bit period decreases. This relationship significantly impacts on the cable length tolerance. For example, if we were

to build the previous Mach-Zehnder coupler (one bit period delay with a tolerance of 2%) that operated at the increased data rate of 200 Mbps, we would need to construct a length fiber that measured 103 ± 2 cm. Doubling the data rate resulted in decreasing by half the margin of error allowed in creating the fiber. As the required data rate continues to increase, eventually it will reach a point where the fiber cannot be constructed to the required specifications and the tolerance of the bit period will need to be increased in order for the construction of the cable to be achievable. The magnitude of acceptable tolerance permitted at a particular data rate before the digital signal is compromised is something that will need to be investigated in future research.

In Chapter III we learned that the quality of the digital signal depended on the inputs to the second coupler having similar losses. In the first configuration, the two signal paths had a difference in signal loss at the second 2x2 coupler of 1.72 dB. This resulted in a poor digital signal (Figure 3.16(b)). When the optical couplers were rearranged resulting in signal loss difference of 0.87 dB, the signal was greatly improved (Figure 3.17(b)). Even though this was only an improvement of 0.85 dB in signal loss over the previous value, the improvement in performance was dramatic. From Figure 3.4 we know that, while couplers are expected to have a minimum of a 3 dB loss, the actual losses varied from 3.5 to 7.7 dB. With each coupler having its own characteristic losses from port to port, it becomes necessary to have each coupler completely evaluated to determine the most favorable arrangement.

We experienced a 10.6 dB signal loss when using the configuration shown in Figure 3.17. The three 2x2 couplers, each with a minimum signal loss of 3 dB, accounted

for 9 dB of the 10.6 dB loss. The loss could be reduced from 10.6 to approximately 7.6 dB if we could identify a different approach for shifting the phase, thereby eliminating the need for the third 2x2 coupler. The signal loss could be further reduced by using fusion splicing to make connection as opposed to using ST connectors. Using fusion splicing, losses as low as several hundredths of a dB are achievable [Ref. 12]. Figure 4.1 illustrates the four positions where fusion splicing would be appropriate.

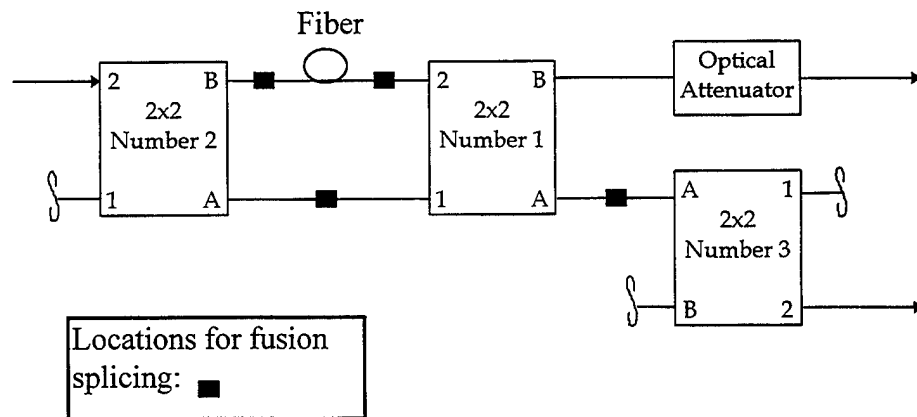


Figure 4.1 Mach-Zehnder coupler showing locations where fusion splicing would benefit Mach-Zehnder coupler.

Before building the Mach-Zehnder coupler, I believed the extra length of fiber was the critical element and that my ability to create that extra length necessary to delay a digital signal by one bit period in relation to another digital signal would determine the quality of the Mach-Zehnder coupler. In the final analysis, I found the fiber at 100 Mbps to be more forgiving than the couplers. I realize that the optical couplers were the key to

the performance of the Mach-Zehnder coupler and the quality of signal was dependent on the ability to achieve similar losses across each signal path.

In conclusion, having built and tested the Mach-Zehnder coupler, we estimate that the signal loss for the Mach-Zehnder receiver, shown in Figure 1.2, will be approximately 21.12 dB (10.6 dB for each stage of the two stage receiver). This loss is significant for a small signal and must be reduced. The loss can be diminished by finding an alternative method for shifting the phase, thereby eliminating the two additional 2x2 couplers which would reduce the loss to 15 dB. The impact of the loss could also be lessened by increasing the signal through adding an optical amplifier to the receiver (before the couplers). Future research should focus on investigating the following:

1. Maximum tolerance allowed for the bit period delay at various data rates.
2. Reduction of the signal losses by fusion splicing the fibers in the couplers.
3. Alternate methods of creating a ninety-degree phase shift without using 2x2 couplers.
4. Construction and testing of the complete receiver.

APPENDIX A. DETAILED DESCRIPTION OF EQUIPMENT AND PROCEDURE USED FOR MEASURING INSERTION LOSSES

The following is a detailed description of the equipment and procedure used (Figure A.1) to measure the insertion loss of the optical fiber, optical 2x2 coupler and optical attenuator.

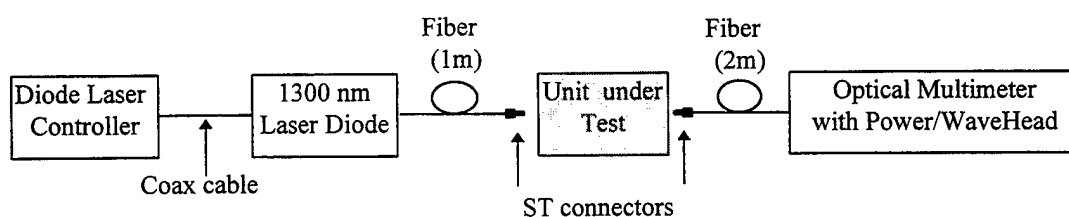


Figure A.1 Block diagram illustrating procedure used to measure insertion losses.

The diode laser controller, manufactured by Melles Griot (model number DLD 103), is menu driven, allowing the user to select the mode of operation (user control of power or current) and then to specify digitally the laser temperature and power (or current) requirements. For these experiments, the controller was set in the power mode (at 0.17 mW) at a laser temperature of 10°C [Ref. 5]. The controller was connected to a 1300 nm laser diode mounted in a standard laser diode test fixture. The output of the laser diode was through a one meter length of single mode fiber fitted with an ST connector. The optical multimeter, manufactured by ILX Lightwave (model number OMM-6810), was equipped with a Power/WaveHead (model number OMH-6725). The Power/WaveHead was designed to simultaneously measure power and wavelength from the laser source, thereby enabling it to automatically calibrate the wavelength-dependent

response of its InGaAs detector. Input to the multimeter was through an FC connector, connected to a two meter length of single mode fiber with an ST connector. The optical multimeter provided a six digit digital display with a linear power range of 0.000 nW to 999.999 W. The multimeter accepted wavelengths from 1040 to 1600 nm and accurately measured power to within $\pm 3.5\%$ and wavelength to within ± 1 nm [Ref. 6].

Prior to each testing, the output of the laser diode was connected directly to the input of the optical multimeter (Figure A.2). This reading was recorded as the input power to the system. Once the input power was determined, the unit under test (2x2 coupler, optical fiber or attenuator) was inserted between the laser diode and the optical multimeter as shown in Figure A.1. The reading from the optical multimeter was then recorded as the output power. Both the input and output power were rounded to the nearest 1/100 mW. The loss was computed as the ratio of input power to output power with the result converted to decibels.

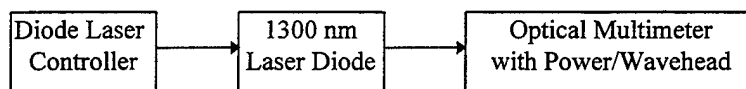


Figure A.2 Block diagram illustrating setup used to measure input power.

APPENDIX B. DETAILED DESCRIPTION OF PROCEDURE USED FOR MEASURING THE TIME DELAY

The following is a detailed description of the equipment and procedure used (Figure B.1) to measure the time delay of the optical fiber, optical 2x2 coupler and the Mach-Zehnder coupler.

The pattern generator manufactured by Hewlett Packard (model number HP 70841B) was capable of producing a random sequence or user programmed pattern with a data rate up to 3 Gb/s. We programmed the generator to produce a repeatable pattern (Figure B.1) at a 100 Mbps [Ref. 7]. The output of the generator was sent through an SMA connector and connected to a 50 ohm coax cable to the BNC input of the laser transmitter. The laser transmitter, manufactured by Broadband Communication Products, Inc. (model 400), accepts digital input signals up to 1.3 Gbps and transmits a 1300 nm optical signal. The optical output was via an ST connector [Ref. 8]. The output of the transmitter was connected to the input port of the coupler under test; then each of the two coupler output ports was connected to a photoreceiver. The optical receivers used were manufactured by New Focus, Inc. (model number 1611). The photoreceiver was an InGaAs PIN photodiode followed by a low noise amplifier. The photoreceiver is equipped with ST connectors for the optical input and an SMA connector for the electrical output [Ref. 9]. The output of the photoreceivers was sent to the digital sampling oscilloscope. The digital sampling oscilloscope, manufactured by Tektronix (model number 11801B), obtained a measurement level accuracy of ± 2 mV. The

oscilloscope is equipped with an SD-14 sampling head which provided dual-channel 3 GHz sampling probes [Ref. 10].

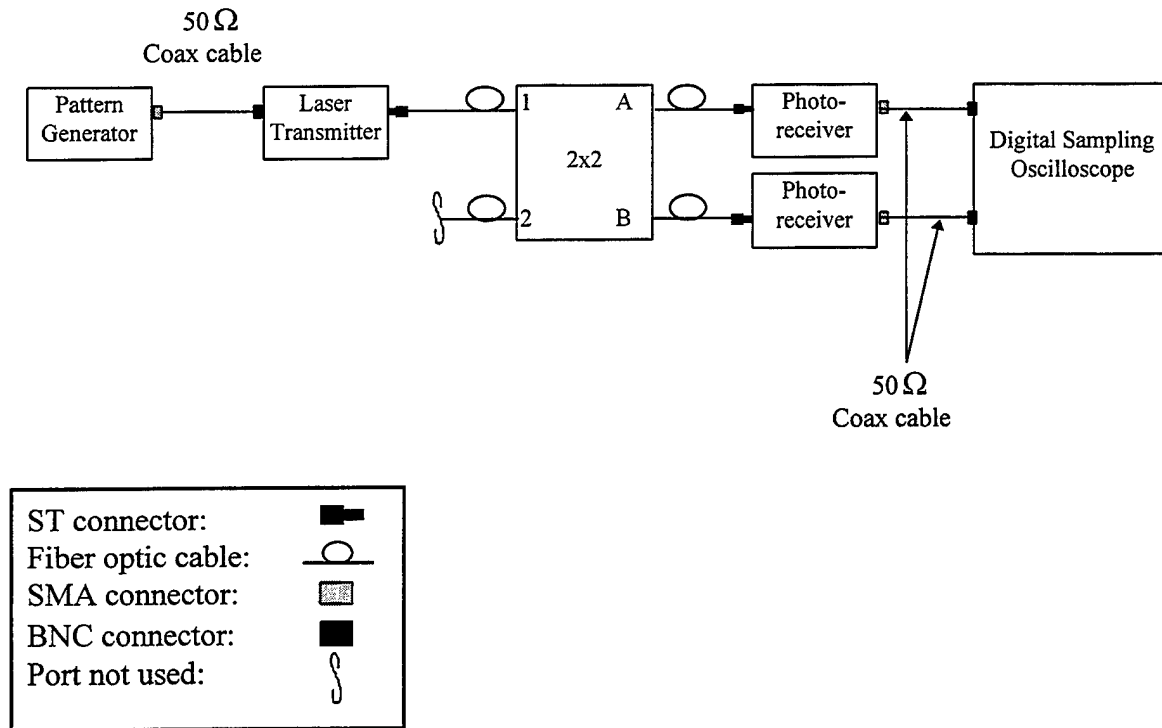


Figure B.1 Block diagram of procedure used to measure time delay.

1100 1010 1010 1010 1010 1010 1010 1010 1000 0000 1000 0000 1000 0000 1000 0000

Figure B.2 Repeatable pattern programmed into the pattern generator.

LIST OF REFERENCES

1. Russell, D and Gangemi, G.T. Sr., *Computer Security Basics*, O'Reilly & Associates, Inc., Sebastopol, CA, 1991.
2. Proakis, J.G., *Digital Communications*, McGraw-Hill, Inc., New York, 1995.
3. Tri Ha, Private communications, Naval Postgraduate School, Monterey CA, 1996-1997.
4. Green, P.E. Jr., *Fiber Optic Networks*, Prentice Hall, Englewood Cliffs, NJ, 1993.
5. Melles Griot, 06DLP103 *Precision Diode Laser Controller Instruction Manual*, Irvine, CA, 1993.
6. ILX Lightwave Corporation, OMH-6725 *InGaAs Power/WaveHead Instruction Manual*, Palo Alto, CA, 1994.
7. Hewlett Packard, HP 71600B *Series of Gbit/s Testers Operating Manual*, Palo Alto, CA, 1992.
8. Broadband Communications Products, Inc., B100021 *Model 400 Laser Transmitter Operators Manual Revision G*, Melbourne, FL, 1993.
9. New Focus Inc., High-Speed Photoreceivers Models 1601 and 1611 User's Manual, 160118 Rev.C., Mountain View, CA.
10. Tektronix Inc., 11801B, *Digital Sampling Oscilloscope*, Beaverton, OR, 1993.
11. Hecht, J., *Understanding Fiber Optics Second Edition*, Sams Publishing, Indianapolis, IN, 1993.
12. Powers, J.P., *An Introduction to Fiber Optic Systems*, Richard D. Irwin, Inc., and Aksen Associates, Inc., Burr Ridge, IL, 1993.

INITIAL DISTRIBUTION LIST

	No. of copies
1. Defense Technical Information Center 8725 John J. Kingman Rd., STE 0944 Ft. Belvoir, VA 22060-6218	2
2. Dudley Knox Library Naval Postgraduate School 411 Dyer Rd. Monterey, CA 93943-5101	2
3. Department Chairman, Code EC Department of Electrical and Computer Engineering Naval Postgraduate School Monterey, CA 93943-5121	1
4. Professor John P. Powers, Code EC/Po Department of Electrical and Computer Engineering Naval Postgraduate School Monterey, CA 93943-5121	2
5. Professor Tri Ha, Code EC/Ha Department of Electrical and Computer Engineering Naval Postgraduate School Monterey, CA 93943-5121	2
6. LT Maryanne Heinbaugh..... 208 Saint Lo Rd. Seaside, CA 93955	1